AN ANALYSIS OF POLISHING FORCES IN MAGNETIC FIELD ASSISTED FINISHING

Vasishta Ganguly[1], Tony L. Schmitz[1], Arthur Graziano[2], and Hitomi Yamaguchi[2]
[1]Department of Mechanical Engineering and Engineering Science
University of North Carolina at Charlotte, Charlotte, NC, USA
[2]Department of Mechanical and Aerospace Engineering
University of Florida, Gainesville, FL, USA

INTRODUCTION

In magnetic field assisted finishing (MAF) a magnetic field is used to maneuver a flexible "magnetic brush" (composed of ferromagnetic particles and abrasives captured in a magnetic field) over the surface to be polished. The relative motion between the brush and the surface can be obtained either by rotating the brush, moving the sample, or both. The brush can consist of either: 1) sintered particles, where the ferromagnetic and abrasive particles (e.g., SiC, Al_2O_3, CBN, or diamond) are sintered together to form a ferromagnetic conglomerate; or 2) separate abrasive and ferromagnetic particles. For the latter case, the abrasives are held between and within the magnetic chains (brush) which are formed. A lubricant can also be used to aid in holding the abrasive particles within the flexible brush. Figure 1 provides a schematic of the material removal process.

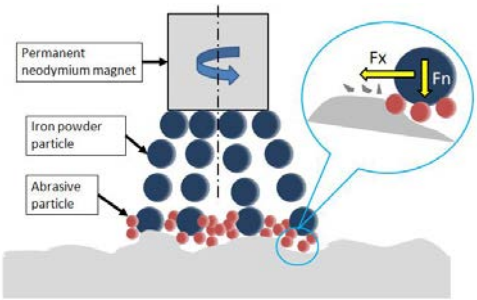

FIGURE 1. MAF process.

In this study, the polishing forces during MAF were examined. The measured forces were divided into forces due to polishing effects and forces due to magnetic effects. A method to identify and isolate the different elements of the force measurement was established. The effect of varying the iron particle size and the working gap on polishing forces and surface roughness was examined. A coherence scanning interferometer (CSI) was used to measure surface roughness. A surface roughness of 2-3 nm Sa was achieved under certain conditions.

EXPERIMENTAL SETUP

The experimental setup consisted of mounting a permanent neodymium magnet in a fixture held in the spindle of a CNC milling machine. The sample was mounted on a ferromagnetic mount which completed the magnetic circuit and strengthened the magnetic field in the gap between the magnet and the sample. This increased the forces on the iron particles within the slurry. The sample was glued to the sample mount using an epoxy resin. The sample-sample mount combination was fixed on a 3D force sensor (Kistler 9256 C1 dynamometer). Each polishing trial consisted of approaching the sample in the normal direction to capture all the magnetic effects. The magnet was then rotated and translated for a fixed period before retracting from the sample. Figure 2 shows a schematic of the experimental setup.

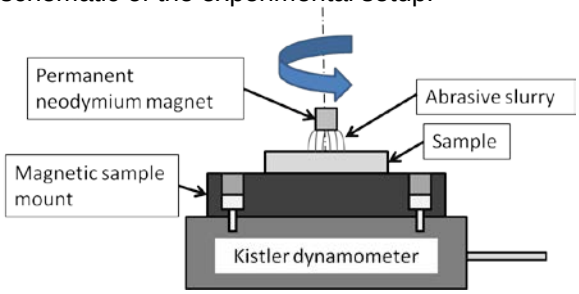

FIGURE 2. Schematic of the experimental setup.

Polishing Forces

The MAF forces can be divided into two categories: 1) magnetic effects; and 2) interactions between the brush and sample. When studying the forces for different polishing conditions, it is important to accurately separate the two categories. The magnetic forces exist mainly due to magnetic interactions between the permanent magnet, the ferromagnetic sample mount, the ferromagnetic slurry and any magnetism the sample may exhibit. Each of

these effects was individually identified using a series of tests. Once the cumulative magnetic effects were evaluated, a reference was computed with respect to which the polishing forces were measured. The individual tests are listed below

A) No Sample, No Slurry

The polishing cycle was completed with no sample or slurry. This enabled the pull of the magnet on the sample mount in the surface normal direction (n) to be isolated.

B) No Sample, With Slurry

The polishing cycle was completed without the sample, but with the slurry. There was still no polishing because the slurry did not make contact with the sample mount. This enabled the effect of the slurry on the normal force to be identified.

C) With Sample, No Slurry

The polishing cycle was completed with the sample, but without the slurry. There was therefore no polishing. This test enabled the extra pull due to the sample to be determined. The individual magnetic effects were then identified using the following relationships.

i) Effect of sample mount:

$F_{sm} = -F_{n(\text{no sample, no slurry})}$

ii) Effect of slurry:

$F_{sl} = F_{n(\text{no sample, slurry})} - F_{n(\text{no sample, no slurry})}$

iii) Effect of sample:

$F_{sa} = F_{n(\text{sample, no slurry})} - F_{n(\text{no sample, no slurry})}$

The reference was then computed using the following relationship.

$\text{Reference} = -F_{sm} - F_{sl} - F_{sa}$

Figure 3 shows a plot of the normal forces for the different tests used to separate the polishing and magnetic forces. The different forces are identified in figure 4.The magnetic forces exist mainly in the normal direction along the axis of the magnet. The symmetry that exists in the two orthogonal directions nullifies the magnetic effects and only polishing forces are observed. Tests were also conducted to evaluate the effect of translational velocity on lateral polishing forces. No significant effects were observed.

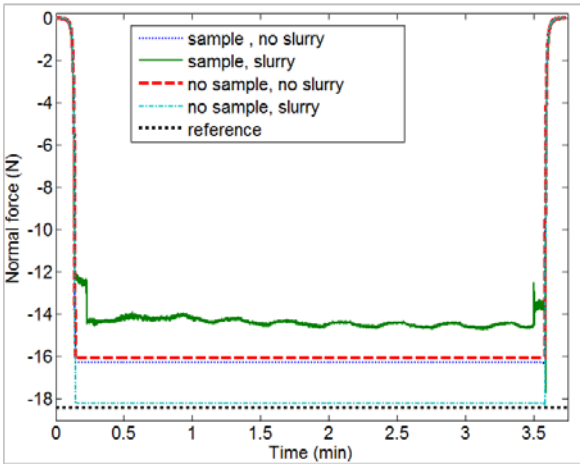

FIGURE 3. Normal polishing forces.

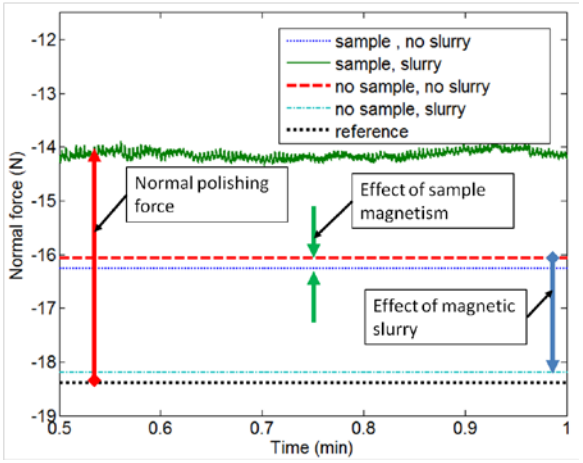

FIGURE 4. Normal force effects.

Surface Roughness

The surface roughness was measured using the CSI at nine different locations on the sample after each polishing trial. Filtering was completed in accordance with ISO 4288. In order to correctly compare the performance of different polishing conditions it was necessary to establish a common starting roughness on all samples. The samples were initially polished using a nylon mesh pad to a consistent surface roughness of 70-90 nm Sa.

RESULTS

Polishing Forces

The normal force magnitude decreased slightly as the iron particle size increased. It is proposed that the smaller iron particles enabled the formation of a more even brush which caused a larger number of particles to be in contact with the sample. Therefore, although the smaller iron particles may experience smaller magnetic field forces individually, on the whole they apply more

attractive force between the magnet and sample resulting in a higher normal force. This effect was also seen in the lateral force measurements. These results are displayed in figure 5.

The normal polishing force exhibited a strong dependence on the working gap. This is because the flux density decreases as the working gap increases. The lateral forces were also inversely related to the working gap. The results are shown in figure 6.

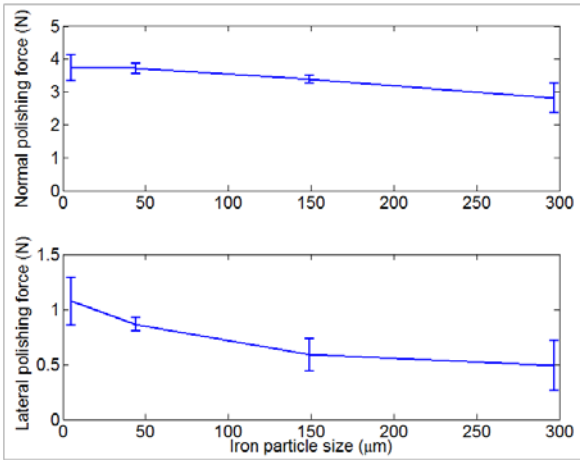

FIGURE 5. Polishing force measurements for varying iron particle size.

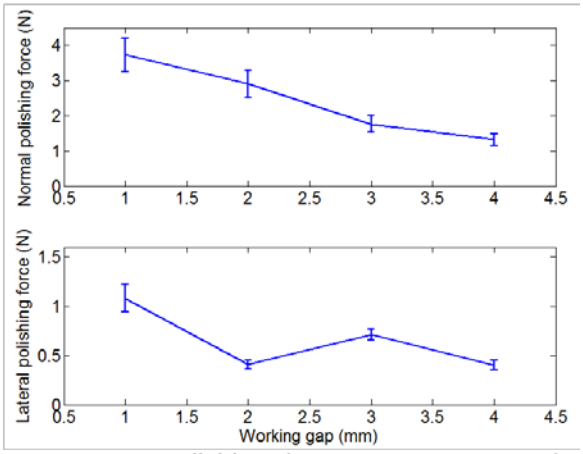

FIGURE 6. Polishing force measurements for varying working gap.

Surface Roughness

There is no material removal when the iron particle size (IPS) is smaller than the top width of the valley. As the IPS increases, the particles are prevented from entering the valleys and produce material removal at the peaks. It is also important to note that, although the entire brush might produce larger normal and lateral forces, each individual particle for the smaller sized iron particles exerts little force on the surface. Thus, the localized polishing force is higher when IPS is greater. This resulted in a faster improvement in surface roughness.

A combination of two factors dictates whether there is material removal: 1) the IPS should be larger than the top width of the valleys in the surface; and 2) the IPS must be large enough to impart sufficient force on the individual abrasive particles to cause material removal. The material removal rate and surface roughness improve significantly for larger IPS (Figure 7). The working gap (WG) was found to have little effect on polishing performance as long as the amount of slurry was maintained proportional to the WG (Figure 8).

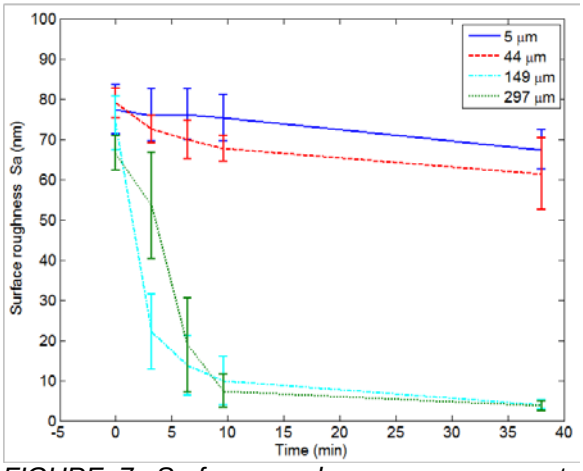

FIGURE 7. Surface roughness measurements for varying iron particle size.

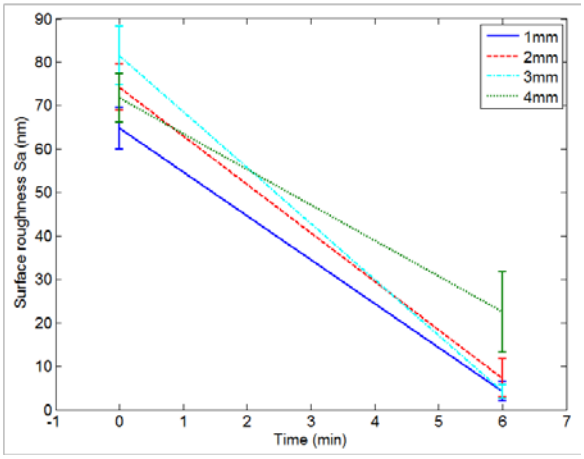

FIGURE 8. Surface roughness measurements for varying iron particle size.

Material Removal Rate (MRR)

The effect of iron particle size on the MRR for MAF was analyzed. The material removed was determined by imaging the sample surface on the CSI before and after polishing. A set of dimples were created on the sample surface using a spherical indenter. The spherical indenter ensured low slopes at the bottom of the indent which made it possible to image the bottom of the indent. These indents were imaged on the CSI to measure the depth of the indent. The bottom of the indent was set as the reference surface with respect to which the material removal rate was then determined. It was assumed that there was no material removal at the bottom of the dimple.

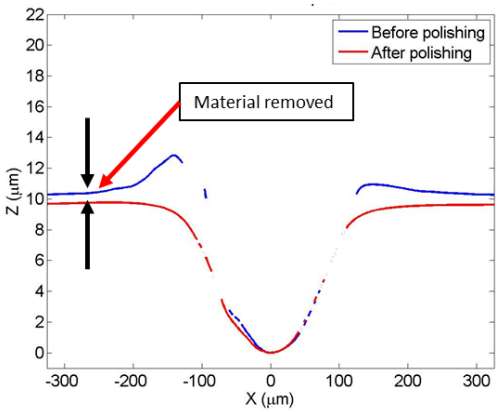

FIGURE 9. Cross-section of dimple.

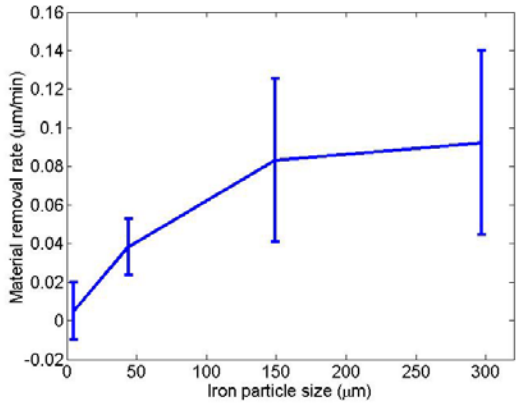

FIGURE 10. Material removal rate for varying iron particle size.

Figure 9 shows the cross-sectional views of the dimple before and after polishing along with a representation of the material removed. The MRR was measured for polishing with different iron particle sizes; see figure 10. The MRR was measured at nine different locations on the sample. The error bars represent one standard deviation in MRR between these nine locations.

Surface Texture

The direction of lay on the polished surface depends on the path of the slurry in contact with the surface. A direct correlation between the direction between the abrasive path and surface texture was observed.

CONCLUSIONS

A number of conclusions can be drawn based on the experimental results and analysis.

1. While measuring MAF polishing forces, it is necessary to isolate the magnetic field effects from the polishing effects.
2. The normal and lateral forces were found to have an inverse relationship with both IPS and WG.
3. The rate of improvement in surface roughness with polishing time depends on the IPS. If the particles are too small, there is little material removal even after polishing for prolonged periods of time. The rate of improvement in surface roughness is not sensitive to WG.
4. The MRR increases considerably with iron particle size.
5. The translational velocity has almost no effect on the magnitude of lateral polishing force.
6. The lay of the polished surface is dictated by the path of the magnetic field and the direction of the abrasive particles.

REFERENCES

[1] Jain, V.K., Magnetic Field Assisted Abrasive based Micro-/Nano-finishing, Journal of Materials Processing Technology, 2009; 209 (20): 6022-6038.

[2] Jayswal, S. C., Jain, V. K., and Dixit, P.M., Modeling and Simulation of Magnetic Abrasive Finishing Process, International Journal of Advanced Manufacturing Technology, 2005; 26 (5-6): 477-490.

[3] Mori, T., Hirota, K., Kawashima, Y., Clarification of Magnetic Abrasive Finishing Mechanism, Journal of Materials Processing Technology, 2003; 143-144: 682-686.

[4] Singh, D.K., Jain, V.K., Raghuram, V., Parametric Study of Magnetic Abrasive Finishing Process, Journal of Materials Processing Technology, 2009; 149: 22-29.